ChemComm

COMMUNICATION

Check for updates

Native-carboxylate-assisted enantioselective C–H annulations with allenes and 1,3-dienes on ferrocene

Devendra Parganiha, [iD] Yagya Dutt Upadhyay, [iD] Sumit Khevariya, [iD] †
Pruthviraj Amar Patil,† Svastik Jaiswal, [iD] Yogesh Dhasmana [iD] and
Sangit Kumar [iD] *

Native carboxylate as a directing group in enantioselective C–H activation results in poor stereodiscrimination, due to dynamic ligand exchange during the enantiodetermining concerted metalation–deprotonation (CMD) step. Herein, we present the synthesis of a new class of chiral ferrocene-fused isochroman derivatives from the readily available native carboxylate functionality. The Pd(II)/MPAA-derived enantioselective C–H activation and intermolecular annulation with allenes and 1,3-dienes afforded structurally diverse ferrocene-fused isochromans with up to 80% yield and 96 : 4 enantioselectivity.
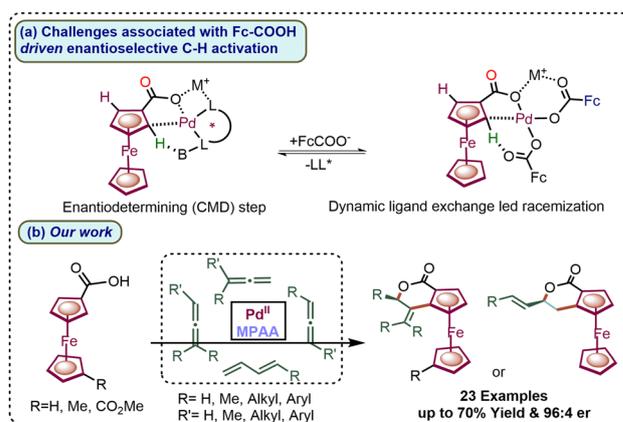
Transition-metal-catalyzed enantioselective C–H activation is a powerful strategy for synthesizing planar chiral ferrocene molecules, with broad applications in both academic research and industrial processes.[1] In this regard, the synthetic utility of the native directing group in planar chiral C–H activation has seen very limited development. The lower enthalpic contribution and conformational flexibility due to native functionalities, such as formaldehydes or carboxylates, lead to rapid ligand exchange.[2] Therefore, methodology enabling highly enantioselective C–H activation using native functionalities is highly challenging.[3] Additionally, a common platform for functional-group-derived enantioselective C–H activation strategy that could enable the synthesis of complex chiral molecules would be highly desirable.[4]

Achieving high enantioselective discrimination in C-sp^3 carboxylate-assisted enantioselective C–H activation is comparatively facile because of the lower rate of dynamic ligand exchange and greater conformational flexibility present around the C-sp^3 carboxylate.[5] However, in the case of enantioselective C–H activation, the use of C-sp^2 attached carboxylate facilitates a rapid ligand exchange equilibrium with chiral ligands, which may lead to racemization (Scheme 1a).[2,6] Consequently, to date,

enantioselective alkenylation *via* FcCOOH-directed C–H activation is achieved with an average of 83% enantioselectivity.[6a]

Planar chiral ferrocene-fused heterocycles represent an important class of molecules that have unlocked new dimensions in the utility and versatility of planar chiral ferrocene scaffolds.[7] However, the synthetic methodologies for these are very limited, as they depend exclusively on pre-designed tethered directing groups.[8] Recently, You and co-workers reported the first Rh-chiral Cp*-enabled amide-directed enantioselective C–H activation followed by intermolecular annulation with alkynes.[9]

Building on these advances, our group also recently demonstrated an amine-enabled enantioselective C–H activation followed by intermolecular annulation on ferrocene.[10] So far, only N-donor directing groups for intermolecular annulations have been reported.[9,11] Herein, we report a Pd(II)/MPAA-enabled methodology for enantioselective C–H activation followed by intermolecular annulation with native ferrocene carboxylate. The regio- and enantioselective intermolecular annulation with allenes and 1,3-dienes afforded a new class of structurally

*Department of Chemistry, Indian Institute of Science Education and Research
Bhopal, Bhopal By-Pass Road, Bhopal, Madhya Pradesh 462066, India.
E-mail: sangitkumar@iiserb.ac.in
† SKK and PP contributed equally.*

Scheme 1 (a) Challenges associated with and the rational development of weak-carboxylate-assisted enantioselective C–H annulations. (b) Our work.

diverse ferrocene-fused isochroman derivatives, achieving yields of up to 80% and 96:4 enantioselectivity (Scheme 1b).

We commenced our investigation using ferrocenecarboxylic acid and allene **2i** with 10 mol% Pd(OAc)$_2$ as a catalyst, 30 mol% ligand (**L1**, Fig. 1), Cs$_2$CO$_3$ as a base, and air as the sole oxidant in the solvent THF. The reaction afforded a 40% yield of ferrocene-fused isochroman **3a** with up to 82:18 er (Table 1, Entry 1). Therefore, to further increase the yield and enantioselectivity, other solvents were screened under the same reaction conditions (Table 1, entries 2–5). *tert*-Amyl alcohol was found to be an efficient solvent for enantioselective synthesis, as it provided a better yield (66%) of **3a** with up to 85:15 er (Table 1, entry 5). The moderate enantiomeric ratio suggested that the rate of ligand exchange may increase with temperature. Therefore, to suppress the ligand exchange, the temperature was lowered to 35 °C. This resulted in an improved reaction outcome, providing **3a** with 70% yield and 90:10 er (Table 1, entry 6). Furthermore, the base Cs$_2$CO$_3$ was replaced with CsF and a slight increment in reaction outcome was observed, affording up to a 75% yield of **3a** and 92:8 er (Table 1, entry 7).

The use of other ligands (**L2–L12**) was also examined under the optimised reaction conditions (entry 7 and Fig. 1), but no further improvement in the reaction was observed. However, it is worth noting that the presence of the –COOH group in the ligand backbone is crucial for achieving enantioselectivity. Other bidentate ligands (**L7–L9, L11**) without –COOH were found to be completely unfit to achieve any chirality (Fig. 1). **L10** also failed to provide any enantioselectivity due to the possibility of 6-membered palladacycle formation. This suggests that the carboxylate group of the chiral ligand may exhibit a κ^2(O,O) mode of binding in the enantio-determining CMD under the reaction conditions.[2] Substituting the amino acid for a chiral phosphoric acid (**L12**) provided an er of only 54:46 (Fig. 1). Furthermore, increasing the loading of Ligand **L1** to 0.6 equiv. provided 80% yield and 93:7 er (Table 1, Entry 8).

Table 1 Optimization of the ferrocene-carboxylate-assisted enantio-selective C–H annulation of allenes^a
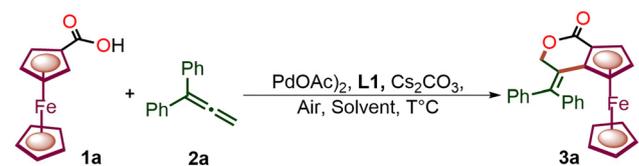
Entry	Solvent	Temp.	3a^b (%)	er^c (%)
1	THF	60	40	82:18
2	Toluene	60	18	60:40
3	DMF	60	NR	NR
4	TFE	60	NR	NR
5	^{t}Amyl Alc	60	66	85:15
6	^{t}Amyl Alc	35	74	90:10
7^d	^{t}Amyl Alc	35	75	92:8
8^e	^{t}Amyl Alc	35	80	93:7

^{a} Reaction conditions: **1a** (0.1 mmol), **2a** (0.2 mmol), Pd(OAc)$_2$ (0.01 mmol), ligand (0.03 mmol), Cs$_2$CO$_3$ (0.2 mmol), solvent (1 mL), air, T °C, 10 h. ^{b} The crude yield of **3a** was determined *via* ^{1}H NMR with CH$_2$Br$_2$ as an internal standard. ^{c} The enantiomeric ratio (er) of **3a** was determined by HPLC analysis. ^{d} 1.5 equiv. of CsF was used instead of Cs$_2$CO$_3$. ^{e} 0.6 equiv. of **L1** was used instead of 0.3 equiv. with 1.8 equiv. CsF.

With the optimized conditions in hand, we next investigated the substrate scope in the developed enantioselective C–H annulation using the native carboxylic acid as a directing group. A wide array of allenes **2b–2k**, including mono-, di-, and tri-substituted variants, were subjected to the reaction to evaluate the versatility of the methodology.

Symmetrical α,α-disubstituted allenes **2b–2d** bearing aryl and alkyl groups participated efficiently in the annulation, affording the corresponding ferrocenyl-fused isochroman derivatives **3b–3d** in good yields (68–70%) with enantioselectivities of 85:15 to 92:8 er (Fig. 2). Encouraged by these results, we turned our attention to unsymmetrical α,α-disubstituted allenes **2e–2h**. These substrates also underwent enantioselective C–H annulation to provide fused isochromans **3e–3h** in good yields and with improved *E*/*Z* selectivity of up to 1:10, along with enantioselectivities ranging from 89:11 to 93:7 er.

Allene **2i** bearing α,γ-di-substitution was also evaluated and provided the desired isochroman **3i** in a moderate yield of 62%. Notably, product **3i** exhibited an outstanding diastereoselectivity of 20:1 (Fig. 2). Furthermore, trisubstituted allenes **2j** and **2k**, which are typically considered to be difficult substrates in transition-metal-catalysed allene functionalization, were evaluated. Gratifyingly, these complex allenes proved to be competent reaction partners, affording the corresponding annulated products (**3j**, **3k**) in moderate yields of 52% and 50%, respectively. Excellent diastereoselectivity of 10:1 and 20:1 dr was observed for **3j** and **3k**. It is worth noting that the corresponding racemic reactions with these di- and tri-substituted allenes resulted in poor regio- and diastereoselectivity, rendering chromatographic separation of isomers challenging. Therefore, enantiomeric ratios for these racemic products could not be reliably determined.

In addition to allenes, phenyl-substituted 1,3-dienes **2l** and **2m** were also successfully employed in the acid-directed C–H annulation. Both substrates delivered the desired products in
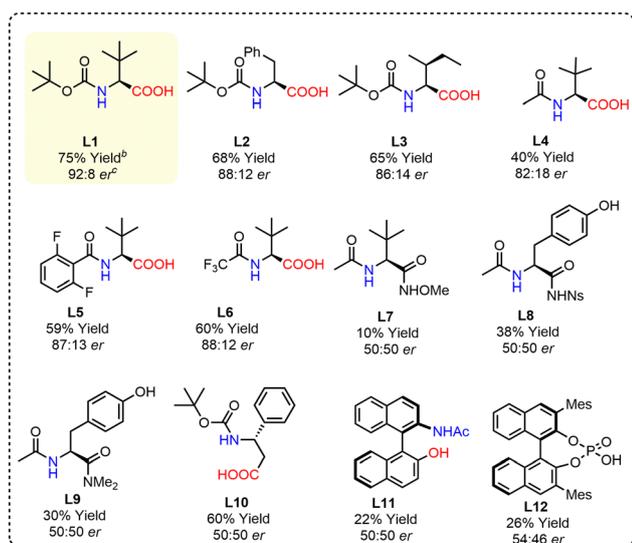

Fig. 1 Screening of ligands for ferrocene carboxylate-assisted enantioselective C–H annulation under the optimized conditions (Table 1, entry 7).
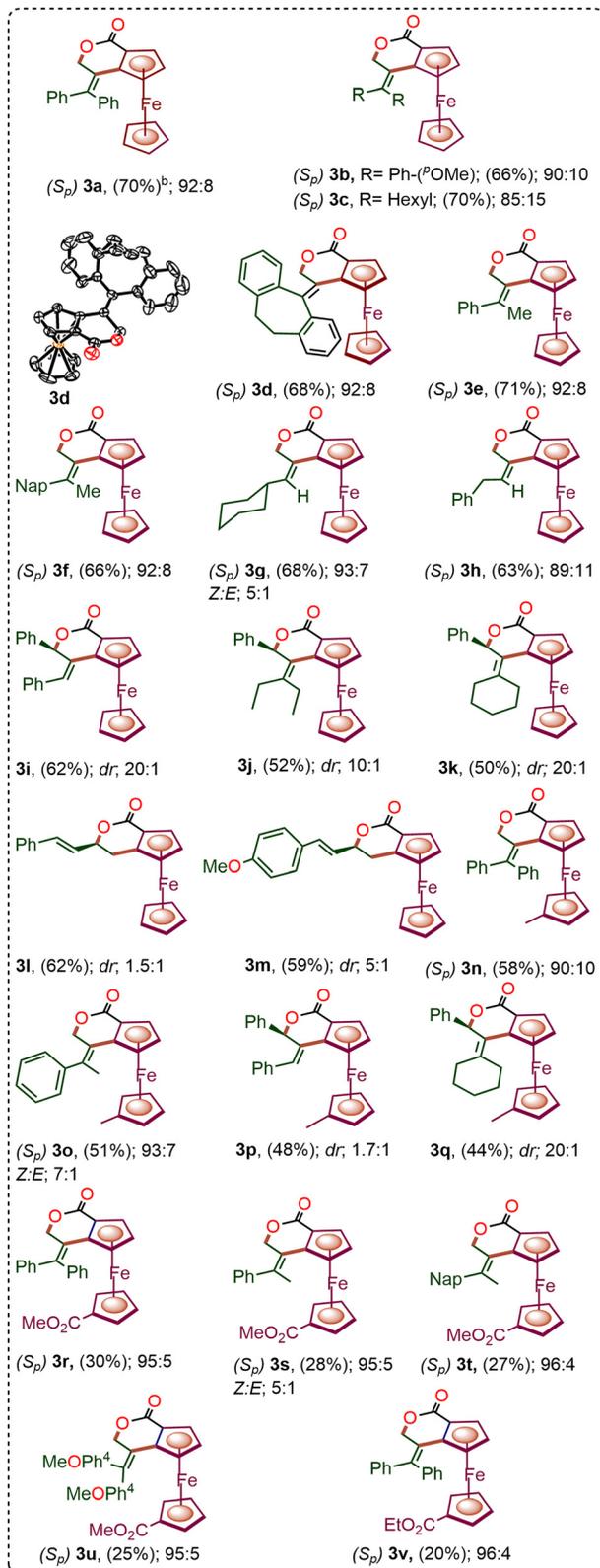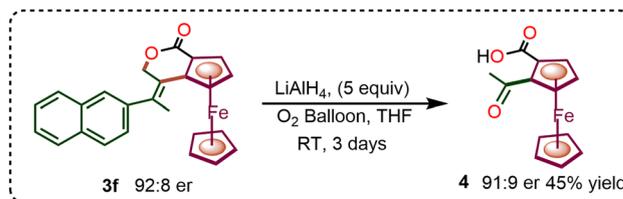
Fig. 2 Substrate scope for the ferrocene-fused isochromans **3a–3v**. [b] Isolated yields for **3a–3v**. Crystal structure of **3d**. The absolute configuration (S_p) assigned based on the crystal structure of **3d**.


Scheme 2 Post-synthetic transformation.

moderate yields of up to 62% with a diastereoselectivity of 1.5 : 1 for **3l** and 5 : 1 for **3m**, respectively. Finally, the scope was extended to structurally modified ferrocene carboxylic acids, with methyl-substituted ferrocenyl derivatives delivering ferrocene-fused isochroman products **3n–3q** in up to 58% yield with excellent diastereoselectivity of 20 : 1 and enantioselectivities of up to 93 : 7 er. Similarly, ester-substituted ferrocenyl substrates underwent annulation to provide **3r–3v** in lower yields (25–30%), albeit with consistently high stereoselectivities of up to 95 : 5 er.

After successfully incorporating diverse allenes and dienes in the enantioselective C–H annulation, we explored post-synthetic transformations of the resulting products. The reduction of compound **3f** with LiAlH$_4$ led to the formation of 1,2-keto acid ferrocene derivative **4** in trace amounts. Upon optimization under an oxygen atmosphere over three days, the yield of compound **4** increased to 45% without any loss of enantioselectivity (Scheme 2). Additionally, the ester-functionalized ferrocene-fused isochroman derivative **3r** underwent selective hydrolysis with NaOH in EtOH at 60 °C for 6 h to afford product **5**.

In the proposed plausible catalytic cycle (Scheme 3), initially, ferrocene carboxylic acid **1a**, Pd(OAc)$_2$ and ligand **L1** with a Cs$^+$ cation form Pd–carboxylate intermediate **I**, which further
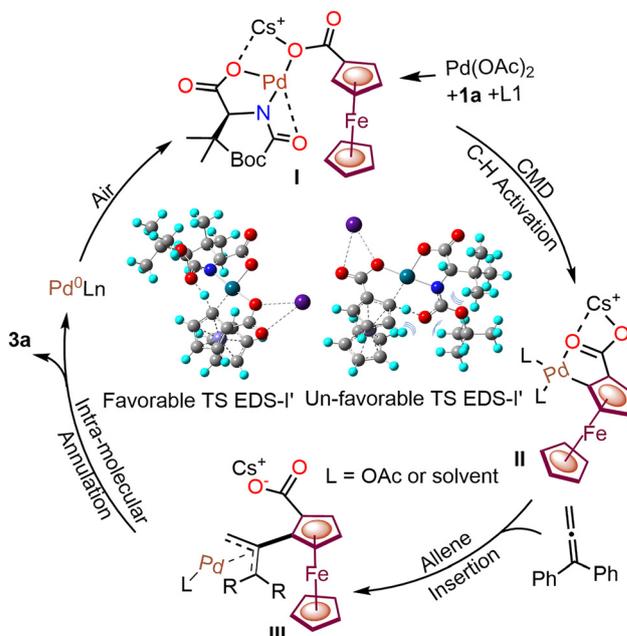
Scheme 3 The catalytic cycle for native carboxylate-assisted enantio-selective C–H annulations with allenes. Favorable and unfavorable transition states are shown (EDS = enantio-determining step).

undergoes enantioselective C–H activation to generate the chiral palladacycle **II**. DFT calculations showed an unfavorable transition state within the enantio-determining step having a 12.0 kcal mol^{-1} higher energy (Scheme 3).

The chiral palladacycle **II** interacts with allenes through π-bond interaction, followed by migratory interaction, leading to the formation of Pd-allyl intermediate **III**.[12] Consequently, intermediate **III** undergoes intramolecular annulation to afford a chiral ferrocenyl-fused isochroman.

In conclusion, we have presented a Pd(II)/MPAA-enabled methodology for enantioselective C–H activation followed by intermolecular annulation with native ferrocene carboxylate. Regio- and enantioselective intermolecular annulation with allenes and 1,3-dienes afforded a new class of structurally diverse ferrocene-fused isochromans, achieving yields of up to 70% and 96:4 er. The isochroman core is very important for facilitating various applications driven by electron transfer phenomena and is currently being explored in our laboratory.

SK and DP designed the research. DP, YDU, SKK, PP, and SJ synthesized all precursors and chiral ferrocene-fused isochroman derivatives. SK did the post-synthetic transformations. YD performed the DFT computational studies. All authors have approved the final version of the manuscript.

Conflicts of interest

There are no conflicts to declare.

Data availability

The data supporting this article have been included as part of the supplementary information. Supplementary information: all the data related to the experimental procedures, theoretical calculation data, characterization data, HPLC analysis data, and copies of NMR spectra of the synthesized chiral ferrocene fused isochromans **3a–3v** and **4**. FAIR data, including the primary NMR FID files, has also been provided as a ZIP file. See DOI: https://doi.org/10.1039/d5cc06160a.

CCDC 2498520 (**3d**) contains the supplementary crystallographic data for this paper.[13]

Acknowledgements

References

1 (a) S. Murai, F. Kakiuchi, S. Sekine, Y. Tanaka, A. Kamatani, M. Sonoda and N. Chatani, *Nature*, 1993, **366**, 529–531; (b) G. Liao, T. Zhang, Z.-K. Lin and B.-F. Shi, *Angew. Chem., Int. Ed.*, 2020, **59**, 19773–19786; (c) R. L. Carvalho, R. G. Almeida, K. Murali, L. A. Machado, L. F. Pedrosa, P. Dolui, D. Maiti and E. N. D. S. Júnior, *Org. Biomol. Chem.*, 2021, **19**, 525–547; (d) R. S. Thombal, P. Yuosef, M. Rubio, D. Lee, D. Maiti and Y. R. Lee, *ACS Catal.*, 2022, **12**, 5217–5230; (e) B. B. Zhan, L. Jin and B.-F. Shi, *Trends Chem.*, 2022, **4**, 220–235; (f) Q. Zhang, L.-S. Wu and B.-F. Shi, *Chem*, 2022, **8**, 384–413; (g) K. Wu, N. Lam, D. A. Strassfeld, Z. Fan, J. X. Qiao, T. Liu, D. Stamos and J.-Q. Yu, *Angew. Chem., Int. Ed.*, 2024, **63**, e202400509.

2 (a) T. A. Stephenson, S. M. Morehouse, A. R. Powell, J. P. Heffer and G. Wilkinson, *J. Chem. Soc.*, 1965, 3632–3640; (b) D. C. Powers and T. Ritter, *Nat. Chem.*, 2009, **1**, 302–309; (c) D. E. Hill, K. L. Bay, Y.-F. Yang, R. E. Plata, R. Takise, K. N. Houk, J.-Q. Yu and D. G. Blackmond, *J. Am. Chem. Soc.*, 2017, **139**, 18500–18503; (d) C. A. Salazar, J. J. Gair, K. Flesch, I. A. Guzei, J. C. Lewis and S. S. Stahl., *Angew. Chem., Int. Ed.*, 2020, **59**, 10873–10877.

3 (a) G. Li, L. Wan, G. Zhang, D. Leow, J. Spangler and J.-Q. Yu, *J. Am. Chem. Soc.*, 2015, **137**, 4391–4397; (b) D. A. Strassfeld, C.-Y. Chen and H.-S. Park, *et al.*, *Nature*, 2023, **622**, 80–86; (c) S. Saha, J. Das, S. A. Al-Thabaiti, S. M. Albukhari, Q. A. Alsulami and D. Maiti, *Catal. Sci. Technol.*, 2023, **13**, 11–12.

4 (a) B.-F. Shi, N. Maugel, Y. H. Zhang and J.-Q. Yu, *Angew. Chem., Int. Ed.*, 2008, **47**, 4882–4886; (b) D. W. Gao, Y. C. Shi, Q. Gu, Z. L. Zhao and S.-L. You, *J. Am. Chem. Soc.*, 2013, **135**, 86–89; (c) L. Chu, K. J. Xiao and J.-Q. Yu, *Science*, 2014, **346**, 451–455; (d) Q. J. Yao, P. P. Xie, Y. J. Wu, Y. L. Feng, M. Y. Teng, X. Hong and B.-F. Shi, *J. Am. Chem. Soc.*, 2020, **142**, 18266–18276; (e) N. Y. S. Lam, K. Wu and J.-Q. Yu, *Angew. Chem., Int. Ed.*, 2021, **60**, 15767–15790; (f) B. Liu, A. M. Romine, C. Z. Rubel, K. M. Engle and B.-F. Shi, *Chem. Rev.*, 2021, **121**, 14957–15074; (g) J. Grover, G. Prakash, N. Goswami and D. Maiti, *Nat. Commun.*, 2022, **13**, 1085; (h) B. B. Zhan, L. Jin and B.-F. Shi, *Trends Chem.*, 2022, **4**, 220–235; (i) J. H. Docherty, T. M. Lister, G. Mcarthur, M. T. Findlay, P. Domingo-Legarda, J. Kenyon, S. Choudhary and I. Larrosa, *Chem. Rev.*, 2023, **123**, 7692–7760.

5 (a) J. Das, D. K. Mal, S. Maji and D. Maiti, *ACS Catal.*, 2021, **11**, 4205–4229; (b) S. Dutta, T. Bhattacharya, F. J. Geffers, M. Bürger, D. Maiti and D. B. Werz, *Chem. Sci.*, 2022, **13**, 2551–2573; (c) E. L. Lucas, N. Y. S. Lam, Z. Zhuang, H. S. S. Chan, D. A. Strassfeld and J.-Q. Yu, *Acc. Chem. Res.*, 2022, **55**, 537–550; (d) D. Q. Phan and J.-Q. Yu, *J. Am. Chem. Soc.*, 2025, **147**, 36999–37004.

6 (a) Y. Huang, C. Pi, X. Cui and Y. Wu, *Adv. Synth. Catal.*, 2020, **362**, 1385–1390; (b) A.-L. Jiang, G. Zhou, B.-Y. Jiang, T. Zhou, X.-T. Xu and B.-F. Shi, *Org. Lett.*, 2024, **26**, 5670–5675.

7 (a) O. Bernardo, S. González-Pelayo and L. A. López, *Eur. J. Inorg. Chem.*, 2021, e202100911; (b) J. Mahrholdt, E. Kovalski, M. Korb, A. Hildebrandt, V. Vrček and H. Lang, *Eur. J. Inorg. Chem.*, 2021, 578–589; (c) S. R. Mohanty, N. Prusty, T. Nanda, P. S. Mahulkar and P. C. Ravikumar, *Org. Chem. Front.*, 2024, **11**, 540–575.

8 (a) M. Ogasawara, S. Watanabe, K. Nakajima and T. Takahashi, *J. Am. Chem. Soc.*, 2010, **132**, 2136–2137; (b) D. W. Gao, Q. Yin, Q. Gu and S.-L. You, *J. Am. Chem. Soc.*, 2014, **136**, 4841–4844.

9 Q. Wang, Y.-H. Nie, C.-X. Liu, W.-W. Zhang, Z.-J. Wu, Q. Gu, C. Zheng and S.-L. You, *ACS Catal.*, 2022, **12**, 3083–3093.

10 (a) R. A. Thorat, D. Parganiha, S. Jain, V. Choudhary, B. Shakir, K. Rohilla, R. K. Jha and S. Kumar, *Org. Lett.*, 2025, **27**, 552–558; (b) D. Parganiha, R. A. Thorat, A. D. Dhumale, Y. D. Upadhyay, R. K. Jha, S. Raju and S. Kumar, *Chem. Sci.*, 2025, **16**, 700–708.

11 (a) X. Vidal, J. L. Mascareñas and M. Gulías, *J. Am. Chem. Soc.*, 2019, **141**, 1862–1866; (b) J. M. González, B. Cendón, J. L. Mascareñas and M. Gulías, *J. Am. Chem. Soc.*, 2021, **143**, 3747–3752; (c) J. M. González, X. Vidal, M. A. Ortuño, J. L. Mascareñas and M. Gulías, *J. Am. Chem. Soc.*, 2022, **144**, 21437–21442; (d) P.-F. Qian, Y.-X. Wu, J.-H. Hu, J.-H. Chen, T. Zhou, Q.-J. Yao, Z.-H. Zhang, B.-J. Wang and B.-F. Shi, *J. Am. Chem. Soc.*, 2025, **147**, 10791–10802.

12 (a) D. Zhao, B. Xu and C. Zhu, *Nat. Commun.*, 2023, **14**, 3308; (b) J. Zhang and C. Zhu, *Angew. Chem., Int. Ed.*, 2025, **64**, e202512977.

13 CCDC 2498520: Experimental Crystal Structure Determination, 2025, DOI: 10.5517/ccdc.csd.cc2pvxfx.